



ARTICLE

Optimizing Hybrid Fibre-Reinforced Polymer Bars Design: A Machine Learning Approach

Aneel Manan¹, Pu Zhang^{1,*}, Shoaib Ahmad² and Jawad Ahmad²

¹School of Civil Engineering, Zhengzhou University, Zhengzhou, 450001, China

²College of Civil Engineering, Tongji University, Shanghai, 200092, China

*Corresponding Author: Pu Zhang. Email: zhpu@zzu.edu.cn

Received: 11 May 2024 Accepted: 06 June 2024 Published: 21 June 2024

ABSTRACT

Fiber-reinforced polymer (FRP) bars are gaining popularity as an alternative to steel reinforcement due to their advantages such as corrosion resistance and high strength-to-weight ratio. However, FRP has a lower modulus of elasticity compared to steel. Therefore, special attention is required in structural design to address deflection related issues and ensure ductile failure. This research explores the use of machine learning algorithms such as gene expression programming (GEP) to develop a simple and effective equation for predicting the elastic modulus of hybrid fiber-reinforced polymer (HFPR) bars. A comprehensive database of 125 experimental results of HFPR bars was used for training and validation. Statistical parameters such as R^2 , MAE, RRSE, and RMSE are used to judge the accuracy of the developed model. Also, parametric analysis and SHAP analysis have been carried out to reveal the most influential factors in the predictive model. Finally, the proposed model was compared to the available equations for elastic modulus. The results demonstrate that the developed GEP model performance is better than that of the traditional formula. Statistical parameters and K-fold cross-validation ensured the accuracy and reliability of the predictive model. Finally, the study recommends the optimal GEP model for predicting the elastic modulus of HFPR bars and improving the structural design of HFPR.

KEYWORDS

Optimization; fiber-reinforced polymer; corrosion resistance; machine learning; hybrid fiber-reinforced polymer; SHAP analysis

List of Nomenclature

FRP	Fiber Reinforced Polymer
HFPR	Hybrid Fiber Reinforced Polymer
GEP	Gene Expression Programming
RMSE	Root Mean Squared Error
MAE	Mean Absolute Error
RRSE	Root Relative Squared Error
R^2	Coefficient of Determination



CFRP	Carbon Fiber Reinforced Polymer
GFRP	Glass Fiber Reinforced Polymer
BFRP	Basalt Fiber Reinforced Polymer
AFRP	Aramid Fiber Reinforced Polymer
ML	Machine Learning
ROM	Rule of Mixture
RoHM	Rule of Hybrid Mixtures
GP	Genetic Programming
GF %	Percentage of Glass Fiber
E-GF	Elastic Modulus of Glass Fiber
CF %	Percentage of Carbon Fiber
E-CF	Elastic Modulus of Carbon Fiber
BF %	Percentage of Basalt Fiber
E-BF	Elastic Modulus of Basalt Fiber
MoE	Modulus of Elasticity
ET	Expression Tree
cos	Cosine
sin	Sine
ln	Natural Logarithm
+	Addition
-	Subtraction
*	Multiplication
/	Division
%	Percentage
avg	Average
kN.m	KiloNewtons.Metre
mm	Millimeter
MPa	Megapascal
GPa	Gigapascal
b_j	Bias
E_c	FRP Bars Modulus of Elasticity
f_r	FRP Bars Tensile Strength
K-FCV	K-Fold Cross Validation
f'_c	Concrete Compressive strength
E_{Hybrid}	Modulus of Hybrid Material
$E_{11,fi}$	Young's Modulus of Fibers
V_{fi}	Volume Fraction of Fibers
E_m	Young's Modulus of Matrix
V_m	Volume Fraction of Matrix
CO ₂	Carbon Dioxide
°C	Degree Celsius
Pi	Predictive Value
Ti	Target Value
∞	Infinity
CV	Cross Validation

1 Introduction

Concrete has high brittleness and low tensile capacity [1]. The introduction of waste materials in concrete provides better durability and strength [2] but still needs to improve tensile reinforcement. Steel reinforced are used to improve the tensile capacity of concrete and ductility. However, reinforced concrete structures have faced various challenges, including steel corrosion, freezing damage in cold climates, and exposure to physical and chemical factors in corrosive conditions [3–6]. In humid environments, air pollutants penetrate through the concrete cover and cause steel reinforcement corrosion. The corrosion of steel within the reinforced concrete results in the expansion of steel, leading to internal cracking, surface cracking, spalling, and failure as shown in Fig. 1 [7].

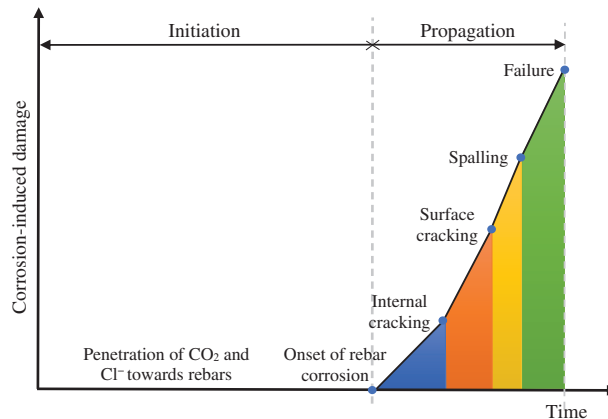


Figure 1: Conceptual model of rebar corrosion process [7]

The reinforcements become exposed to direct environmental attack which accelerates corrosion. The corrosion decreased the overall load-bearing capacity of the structures due to decreased bonds between the steel and concrete. The deterioration not only compromises the structural performance but also demands costly repairs and maintenance [8]. A study also noted that the corrosion of steel strands significantly the serviceability of prestressed concrete structures [9]. Similarly, a study [10] noted that fiber rope has many advantages as compared to steel in marine engineering. Therefore, it is necessary to adopt alternative materials as a solution to overcome the corrosion-related problems of traditional reinforcement. The research proposed different ways to decrease the corrosion of steel. A practical solution involves substituting steel bars with non-corrosive reinforcement materials such as fiber-reinforced polymer (FRP) bars.

Fiber-reinforced polymer (FRP) composites are creative and innovative ideas for addressing the growing problem of infrastructure [11]. FRP bars are promising alternative bars to steel reinforcement due to their high corrosion resistance and high strength properties [12]. Furthermore, FRP (carbon fiber-reinforced polymer) also improved seismic performance [13]. Studies show the anti-degradation performance of FRP bars in corrosive environments. Guo et al. [14] studied the degradation of carbon fiber-reinforced polymer (CFRP), glass fiber-reinforced polymer (GFRP), and basalt fiber-reinforced polymer (BFRP) in sea sand concrete. Results showed CFRP has the highest durability, followed by GFRP, BFRP, and steel. Li [15] explored CFRP and GFRP bars as replacements for steel reinforcement in sea sand concrete. The test findings indicated that the addition of CFRP greatly improves the shear capacity of beams without shear reinforcement, exceeding its effect on beams with appropriate shear reinforcement [16]. The study revealed differing corrosion resistance due to resin matrix dissolution in FRP bars. However, FRP bars demonstrate superior corrosion resistance to steel bars. Nevertheless, FRP bars have a lower elastic modulus than steel bars, and their brittleness is typically caused by their linear stress-strain behavior. Abdalla [17] developed simple methods to

estimate deflection in FRP-reinforced concrete members under flexural stress, highlighting the brittle behavior of CFRP-reinforced beams. Ferreira et al. [18] analyzed simply supported concrete beams reinforced with composite rebars, comparing the effects of reinforcement with composite and steel rebars on concrete. A study [19] reported that hybrid fiber-reinforced concrete (HFRC) shows better performance in terms of tensile and flexural capacity. Recently, GFRP bars have been utilized in various structural elements to investigate their behavior. Chaallal et al. [20] investigated the glass-fiber plastic rods as rebars in concrete structures, focusing on rod characterization, bond performance, and flexural behavior in concrete beams. Results indicate satisfactory performance of concrete beams with glass-fiber rebars compared to steel rebars. However, more cracking under moderate to high loading was observed. Numerous investigations on concrete beams reinforced with FRP bars have been carried out [21–24], and it has been found that using FRP bars enhanced the durability of FRP-reinforced structures [25–27]. However, FRP-reinforced structures often exhibit lower serviceability due to the lower modulus of elasticity and reduced ductility of FRP compared to those reinforced with steel bars [28,29].

The types of FRP bars that are commercially available are CFRP, GFRP, BFRP, and aramid (AFRP). Each FRP bar possesses distinct tensile strength, Young's modulus, ductility, and other characteristics depending on the type of fiber used [30]. Certain types of bars are relatively expensive to produce, and other varieties do not meet the strength requirements. The development of hybrid fiber-reinforced polymer (HFRP) bars presents an optimal solution. HFRP bars have shown significant attention due to their potential for enhanced mechanical properties.

Previous researches Hayashi [31], Belarbi et al. [32], and Ali et al. [33] have highlighted the importance of achieving specific characteristics in HFRP bars, particularly ductility under tensile load and variation of the modulus of elasticity through hybrid fiber configurations. However, experimental studies Bakis et al. [34], Cui et al. [35], You et al. [36], and Harris et al. [37] suggest that more efficient and cost-effective methods are required to optimize the design of HFPR bars. Table 1 [38] illustrates a comparison between machine learning (ML) models and traditional methods, focusing on different aspects such as computational cost, working mechanism, and model applicability. Studies [39–41] reported that ML is a cheaper, more efficient, and alternative approach to the traditional approach.

Table 1: Comparison between ML and traditional models [38]

Type	Machine learning	Traditional methods
Computation cost	Medium	Low
Model structure	Complex	Simple
Working mechanism	Complex	Simple
Model accuracy	High	Low
Limitation	Low	High
Feasibility	High	Low

To optimize cost and time efficiency in the construction industry, ML techniques are being increasingly used to precisely predict various properties [42]. A study [43] concluded that the random forest model shows better accuracy than the back propagation neural network (BPNN) ML model. A study [44] applied machine learning approaches, such as adaptive neuro-fuzzy inference systems (ANFIS), artificial neural networks (ANN), and gene expression programming (GEP), to forecast the compressive strength (CS) of steel fiber-reinforced concrete (SFRC) under high temperatures. The findings indicate that the GEP model has high accuracy and the lowest error in comparison to the ANN and ANFIS models. However, a study [45] predicted the split tensile strength of fiber-reinforced recycled aggregate concrete. Five prediction models namely two deep neural network models (DNN1 and DNN2), one optimizable Gaussian process regression (OGPR) model, and two genetic programming-based models (GEP1 and GEP2) are apply for analysis. The results indicate that all the models demonstrated high accuracy in predicting split tensile strength. The DNN2 model shows highest R^2 value 0.94, while the GEP1 model shows lowest R^2 value 0.76. The R^2 value of the DNN2 model was 3.3% and 13.5% greater than the R^2 values of the OGPR and GEP2 models, respectively. Therefore, a more detailed study is required on GEP to improve its accuracy.

Traditional regression models show lower computational costs due to their dependence on individual parameters for accuracy. However, several factors like hyperparameter tuning and model structure impact the predictive performance of ML models. These factors increase the computational cost and complexity of work than traditional methods. However, traditional models primarily rely on individual sample fittings, resulting in significantly lower prediction accuracy than ML models. Therefore, this study focuses on utilizing GEP, an advanced machine learning technique, to develop HFRP bars that can fill the gap by providing a systematic approach to design optimization, potentially offering improvements in mechanical performance, cost-effectiveness, and time efficiency compared to traditional experimental methods. The proposed approach reduces the limitations of conventional methods and offers an advanced methodology for predicting mechanical properties which bridge the gap between theory and practice. Integrating machine learning techniques into materials science holds significant potential for future advancements in structural design and engineering optimization.

2 Research Methodology

The methodology of this research is described in this section and the steps can be visualized in Fig. 2. Initially, the data was collected from previous published research articles and influential variables were defined. Afterward, the collected data underwent screening to process in which dependent and independent variables statistical analysis is conducted. For the utilization of ML approaches, the data was split into training and testing datasets. Subsequently, GEP algorithms were then employed to develop a highly accurate predictive model, and the best models were selected based on statistical parameters. Validation of the model was carried out. Furthermore, the proposed model was compared with the traditional method to assess robustness and accuracy. The conclusion recommends the most accurate model based on the comprehensive evaluation.

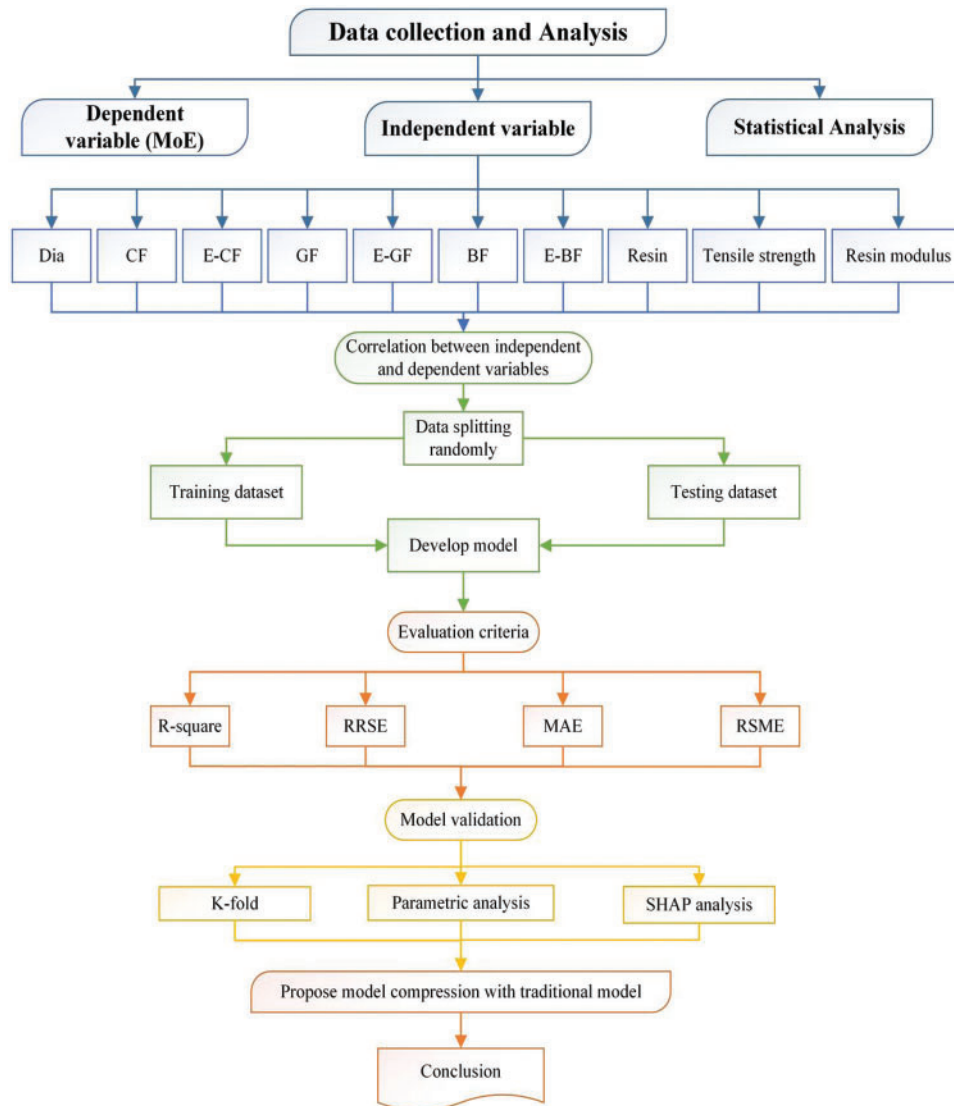


Figure 2: Research methodology

3 Existing Analytical Approach

There are various micromechanical models available in literature with differing accuracy and complexity including Halpin Tsai and rule of mixture (ROM) models. The ROM models are more often utilized as it is relatively simple and yield acceptable prediction values compared to experimental values. Andersons et al. [46] investigated the strength and stiffness of flax fiber composite under uniaxial tension using thermoset and thermoplastic polymer matrices. The study assesses the suitability of orientational averaging-based models and ROM models, originally developed for short fiber composites, to flax-reinforced polymer. Affdl et al. [47] concluded that the Halpin-Tsai equation is preferred for predicting the accuracy of short random fiber composites. Sandier et al. [48] studied the Cai-Pagano equation, which determines longitudinal and transverse modulus to assess composite stiffness, concluding that mixing rules for equations of state enables accurate predictions. Tham et al. [49] have conducted a detailed study on the ROM models, concluding that they assume homogeneity and neglect variations, interfacial effects, and non-linear behavior, thereby indicating

limitations in accurately predicting composite properties. Eq. (1) presents the mathematical model of ROM used to estimate the mechanical properties of composite materials based on their individual components' properties.

$$E_{Hybrid} = \sum_i E_{11,fi} V_{fi} + E_m V_m \quad (1)$$

where E_{11} is Young's modulus of fibers along the longitudinal axis; V_{fi} is the volume fraction of fibers; E_m is Young's modulus of the matrix and V_m is the volume fraction of the matrix. Table 2 reviews mixing approaches for composite materials, revealing inconsistent predictions with experimental values [50–61]. It emphasizes the need for improved mixing equations and alternative approaches in composite materials research.

4 Gene Expression Programming (GEP)

Genetic Algorithms (GA) are optimization and search algorithms inspired by genetics [62–65]. Genetic Programming (GP) was developed by Cramer in 1985 and enhanced by Koza [66,67]. In GP, an initial population of programs with terminals and functions is provided. Functions play a crucial role in program excitation and defining terminals [68,69]. GEP introduced by Candida Ferreria mimics living organisms and involves generating complex tree-like structures/models. GEP considers input variable shapes, compositions, and sizes to search for optimal solutions. It leverages computational intelligence and genetic programming principles rooted in Darwin's and Mendel's theories [70,71].

In GEP, a linear chromosome encodes multiple computer programs, offering advantages like accurate predictive models and robust mathematical expressions [72]. In civil engineering, GEP models are increasingly popular for predictive equations, utilizing generated mathematical formulas. GEP has been successfully applied in structural engineering, predicting concrete parameters [73–77] strength characteristics of steel slag [78], prediction of compression strength of geopolymer concrete [79], determining the nominal shear capacity of steel fiber beam [80], etc. Additionally, GEP modeling is widely used for predicting functions, data mining pattern detection, and equation solving [81].

The GA and GEP work mechanism shown in Figs. 3 and 4 involve generating random generation of chromosomes using the Karva language. A typical chromosome or gene in gene expression programming (GEP) consists of two parts: a head and a tail. The head contains function or terminal symbols, while the tail includes only parameters. The number of genes determines the number of sub ETs in the model. Chromosomes have fixed lengths and can be simply transformed into an algebraic expression [82]. Each GEP gene is composed of a fixed length list of terms, with each term derived from a set of functions. These functions can include arithmetic operations (e.g., +, −, ×, /), Boolean logic functions (e.g., AND, OR, NOT, etc.), mathematical functions (e.g., cos, sin, natural log), conditional functions (e.g., IF, THEN, ELSE), or others [83].

Table 2: Composite material mixing approaches and outcomes in various research studies

Ref.	Study focus	Research center	Purpose/Application	Composite material	Mixing approach	Outcomes
[50]	Mechanical properties of pineapple leaf fiber-reinforced polypropylene composites	Malaysia Nuclear Technology Research (MINT).	Enhancing mechanical properties	Pineapple leaf fiber, Polypropylene (2.7, 5.4, 10.8, and 16.2%)	1. Rule of Mixtures (ROM) 2. $(E_c = E_f V_f + V_m E_m)$	The experimental data revealed that the measured values were consistently lower than the theoretical predictions.
[51]	Interfacial and mechanical properties of environment-friendly "green" composites made from pineapple fibers and poly (hydroxybutyrate-co-valerate) resin	Fibre science program, Cornell University, Ithaca, USA.	Development of environment-friendly composites	Pineapple fiber, Poly (hydroxybutyrate-co-valerate) resin (20 and 30%)	1. Rule of Mixtures (ROM) 2. $(E_c = E_f V_f + V_m E_m)$	The results indicate that the calculated theoretical values tend to be higher than the values observed in the experiments.
[52]	Effect of temperature on tensile properties of injection molded short glass fiber and glass bead-filled ABS hybrids	London Metropolitan Polymer Centre, London Metropolitan University, UK.	Effect of temperature on tensile properties of injection molded short glass fiber and glass bead-filled ABS hybrids	Chopped E-glass fibers/Spherical glass bead/ABS (5:5:90, 5:15:80, 10:10:80, 15:15:70, 20:20:60)	1. Rule of Mixtures (ROM) 2. $(E_c = E_f V_f + V_m E_m)$	It was found that the rule-of-mixtures for hybrids provided an excellent description of the experimental results.
[53]	Stiffness prediction of hybrid kenaf/glass fiber reinforced polypropylene composites using the rule of mixtures (ROM) and rule of hybrid mixtures (RoHM)	Mechanical and Manufacturing Engineering, University of Putra, Malaysia.	Prediction of the stiffness properties (specifically for hybrid composites) based on the combination of kenaf and glass fibers	Hybrid kenaf/glass fiber reinforced polypropylene composites	1. Rule of Mixtures (ROM) 2. Rule of Hybrid Mixtures (RoHM) 3. Tsai-Pagano equations	The ROM and Tsai-Pagano equations aligned well with theoretical claims. The RoHM equation results showed a negative hybrid effect on stiffness. RoHM were closer to the experimental values but tended to slightly overestimate the properties of the composite.
[54]	Prediction of tensile properties of hybrid-natural fiber composites	Mechanical Engineering, Anna University, Chennai, India.	Predicting tensile properties of hybrid composites	Banana/sisal fibers (40:0, 30:10, 20:20, 10:30, 0:40)	1. Rule of Hybrid Mixtures (RoHM) $(E_c = E_f V_f + V_m E_m)$	(Continued)

Table 2 (continued)

Ref.	Study focus	Research center	Purpose/Application	Composite material	Mixing approach	Outcomes
[55]	Effects of fiber length on tensile strength of carbon/glass fiber hybrid composites	Engineering Faculty, Gifu University, Yanagido, Japan.	Evaluate the tensile strength of hybrid composites	Carbon fiber/Glass fiber (1.0:0, 0.5:0.5, and 0:1.0)	1. Rule of Hybrid Mixtures (RoHM)	The experimental results closely match the calculated values, confirming the effectiveness of the hybrid mixtures rule in predicting tensile strength.
[56]	Mechanical properties of polypropylene matrix composites reinforced with natural fibers	Material Engineering Centre, University of Perugia, Italy.	Enhancing mechanical properties of polypropylene composites	Linum usitatissimum fiber/Polypropylene matrix	1. Halpin-Tsai 2. Tsai Pagano 3. Rule of Mixtures (ROM)	The theoretical modal values obtained using these equations are slightly greater than the experimental values measured.
[57]	Tensile properties of wood flour/kenaf fiber polypropylene hybrid composites	The Research Forest of the Natural Resources Faculty, University of Tehran, Iran.	Evaluating tensile properties of the hybrid composites	Wood flour/kenaf fiber polypropylene hybrid composites (40:0, 30:10, 20:20, 10:30, 0:40)	1. Rule of Hybrid Mixtures (RoHM) 2. Halpin-Tsai	The RoHM equation shows a linear trend for its predicted values, and all predicted values are higher than the experimental ones. However, the Halpin-Tsai equation exhibits a different nonlinear trend.
[58]	On the elastic modulus of hybrid particle/short fiber/polymer composites	MEEEM Department, University of Hong Kong, China.	Study the elastic modulus behavior	Glass fiber/Acrylonitrile butadiene styrene	1. Laminar Analogy Approach (LAA) 2. Rule of Hybrid Mixtures (RoHM)	Based on the analysis of previous experimental results, the predicted results of the RoHM equation for the elastic modulus consistently underestimated the values, while the predictions of LAA aligned well with the experimental results.

(Continued)

Table 2 (continued)

Ref.	Study focus	Research center	Purpose/Application	Composite material	Mixing approach	Outcomes
[61]	Predictions of Young's modulus of short inorganic fiber-reinforced polymer composites	Research Division of Green Function Material and Equipment, University of Technology, Guangzhou, China.	To provide valuable insights and predictive tools	Short Glass Fibre/ Polypropylene (2.5%, 5%, 10% and 15%)	1. Liang's equation	The study indicates that the equation is a reliable tool for estimating the mechanical properties of short inorganic fiber-reinforced polymer composites.
[60]	Analysis of the tensile modulus of polypropylene composites reinforced with stone groundwood fibers	Chemical Engineering, University of Girona, Spain (Polypropylene: Eastman Chemical Products, Spain, and Stone groundwood fiber: Vetrotex, Chambéry Cedex, France).	To analyze the effect of fiber content on tensile modulus	Stone groundwood fibers/ Polypropylene (20%, 30%, 40% and 50%)	1. Cox-Krenchel model 2. Halpin-Tsai model 3. Tsai-Pagano equation	The Tsai-Pagano equation provides stiffness predictions that are more closely aligned with the experimental values compared to the Cox-Krenchel model and Halpin-Tsai model.
[59]	Predicting the elastic modulus of natural fiber-reinforced thermoplastics	Department of Chemical Engineering and Applied Chemistry, University of Toronto, Canada.	To predict the elastic modulus of the composite material	Hemp fibers, Hardwood fibers, rice hulls, and E-glass fibers/ High-density polyethylene (10%, 20%, 30%, 40%, 50%, and 60%)	1. Rule of Mixtures 2. Halpin-Tsai Model 3. Mori-Tanaka Model 4. Shear-lag mode	ROM and IROM equations: These equations offer reasonable stiffness prediction bounds. Halpin-Tsai equation: Effective for composites reinforced with glass fibers, but not suitable for composites containing natural fibers. Shear-lag equations by Nairn and Mendel: Consistently overestimate tensile modulus and inadequately represent composites with staggered fiber distribution in a matrix.

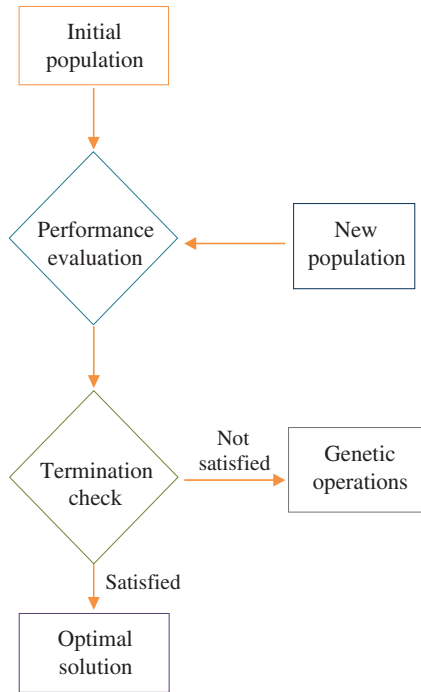


Figure 3: GA flowchart

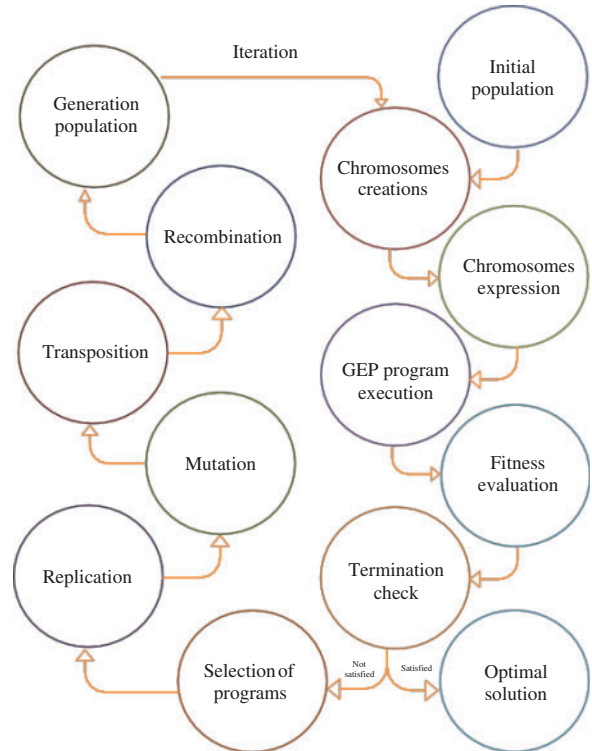


Figure 4: Algorithm of GEP

Afterward, the chromosomes are represented by expression trees (ETs) that come in various shapes and sizes. Then, the main genetic operators such as crossover, mutation, transposition and recombination (including 1-point, 2-point, and gene recombination) are executed on the chromosomes based on their ratios [84]. The ETs are then expressed using karva notation or K-expression [85]. The entire process concludes once the stopping condition (highest number of generations or suitable solution) is met.

5 Data Acquisition and Model Development

5.1 Data Acquisition

In this research, a dataset of 125 values is considered for the GEP and ROM prediction model for HFRP elastic modulus. The data section 1–11 is acquired from [70], data section 12–23 [86], data section 24–25 [87], data section 26–38 [88], data section 39–46 [89], data section 47 [90], data section 48–65 [91], data section 66–106 [92], data section 107–112 [93], data section 113–118 [94], and data section 119–125 [95]. In the current study, 100 data points for training and 25 data points for testing were considered for the generation of the GEP model. Moreover, ten input variables and one dependent variable were taken, i.e., the Diameter of the bar (Dia of the bar), percentage of glass fiber (GF), the elastic modulus of glass fiber (E-GF), percentage of carbon fiber (CF), the elastic modulus of carbon fiber (E-CF), percentage of basalt fiber (BF), elastic modulus of basalt fiber (E-BF), percentage of resin (Resin), tensile strength of resin elastic and modulus of resin (Resin Modulus) against HFRP elastic modulus. The statistical analysis and frequency distribution of the database are shown in Table 3 and Fig. 5, respectively. These are highly dependent variables for governing the elastic modulus of HFRP bars which are collected from previous studies.

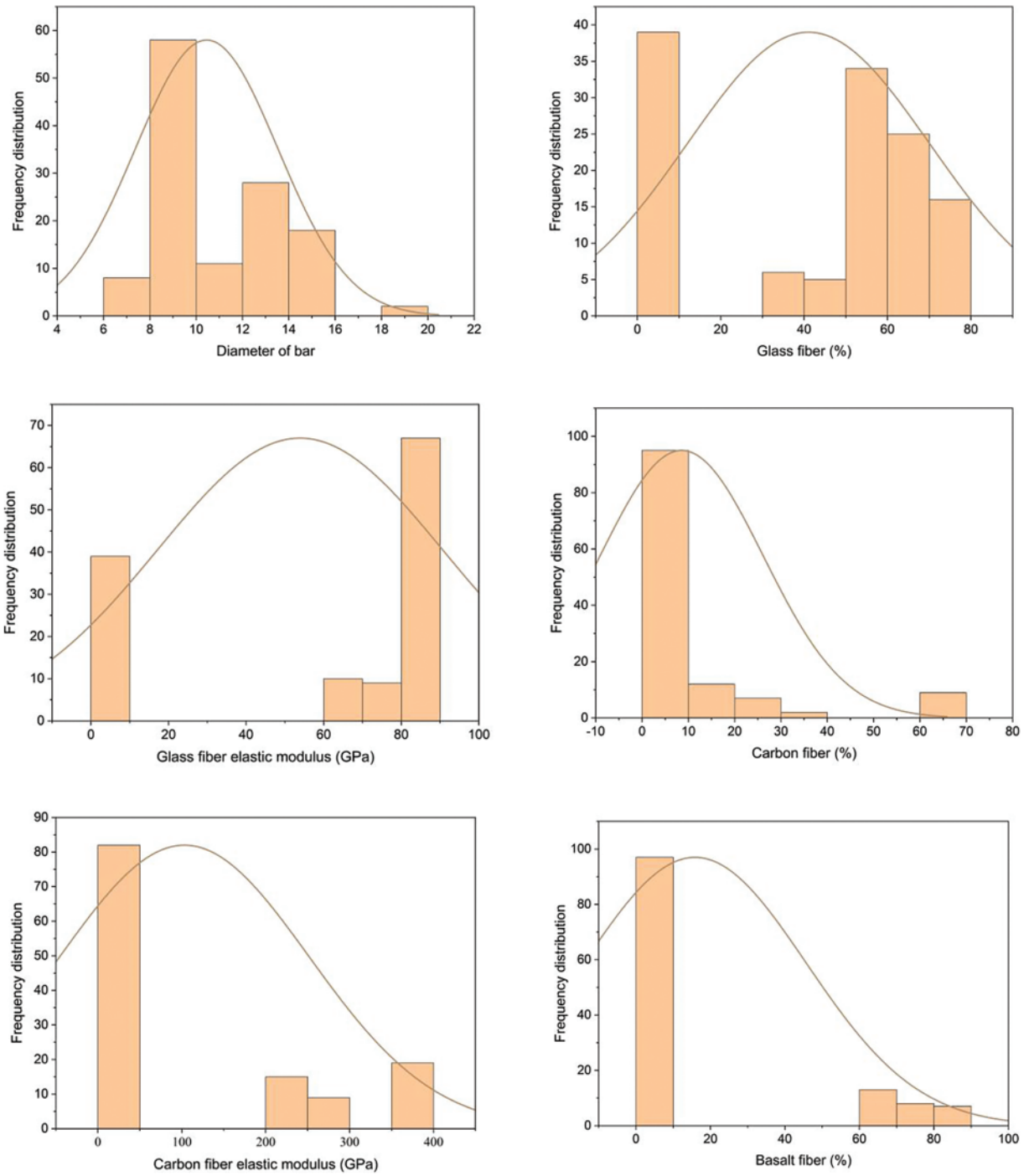


Figure 5: (Continued)

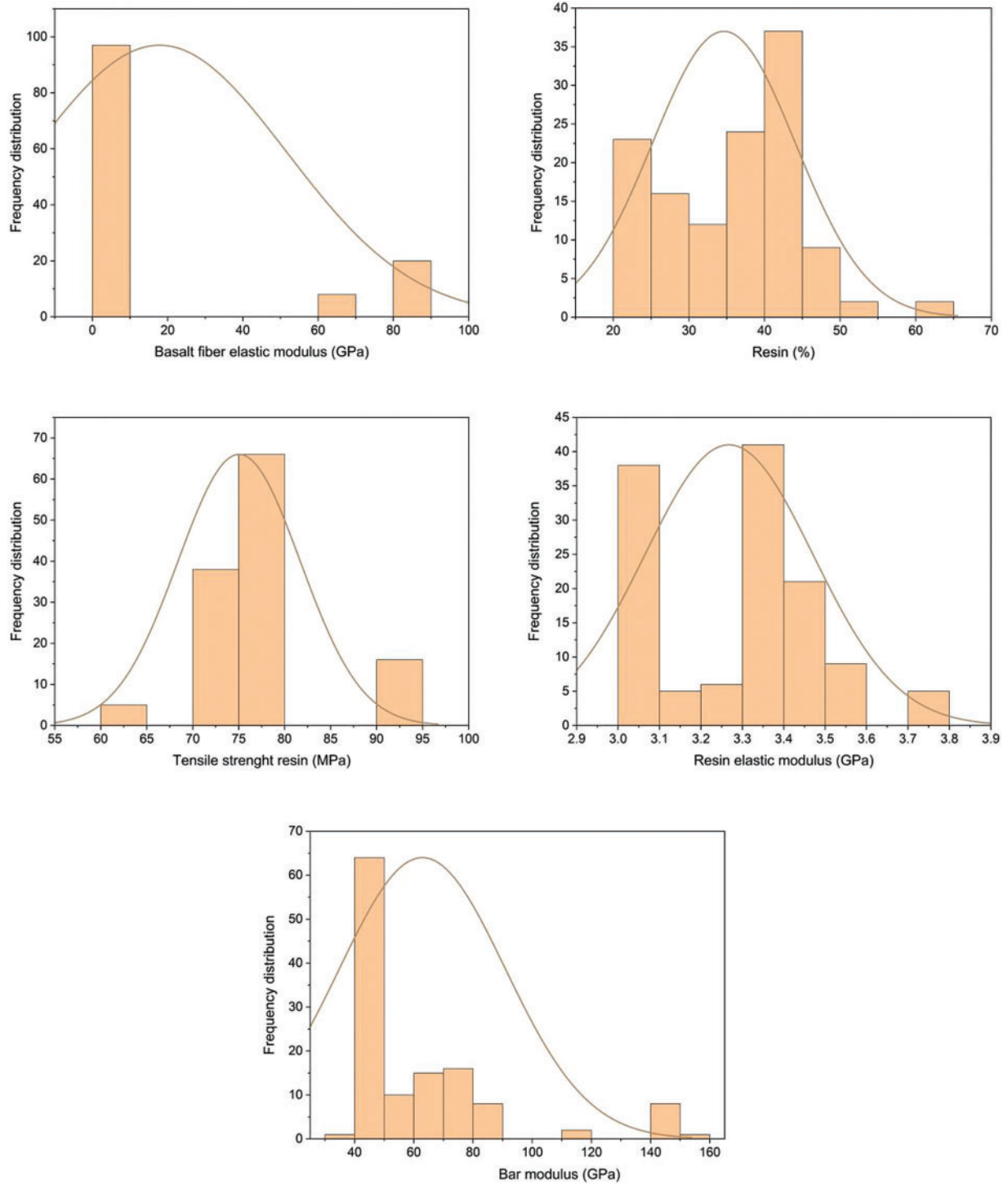


Figure 5: Frequency distribution

Moreover, the study explores the relationships between various variables, as shown in Fig. 6. The results indicate that “GF%” has a positive correlation with “Bar Dia” and “E-GF” (correlation coefficients of 0.301 and 0.311, respectively). This suggests that an increase in glass fiber percentage or effective glass fiber is connected to a larger bar diameter. Additionally, the correlation coefficients

reveal connections among resin properties. Specifically, “Resin%” exhibits a positive correlation with “Resin Tensile Strength” (correlation coefficient: 0.0327) and “Resin Modulus” (correlation coefficient: 0.0688). These correlations indicate that an increase in resin percentage is linked to higher tensile strength and modulus.

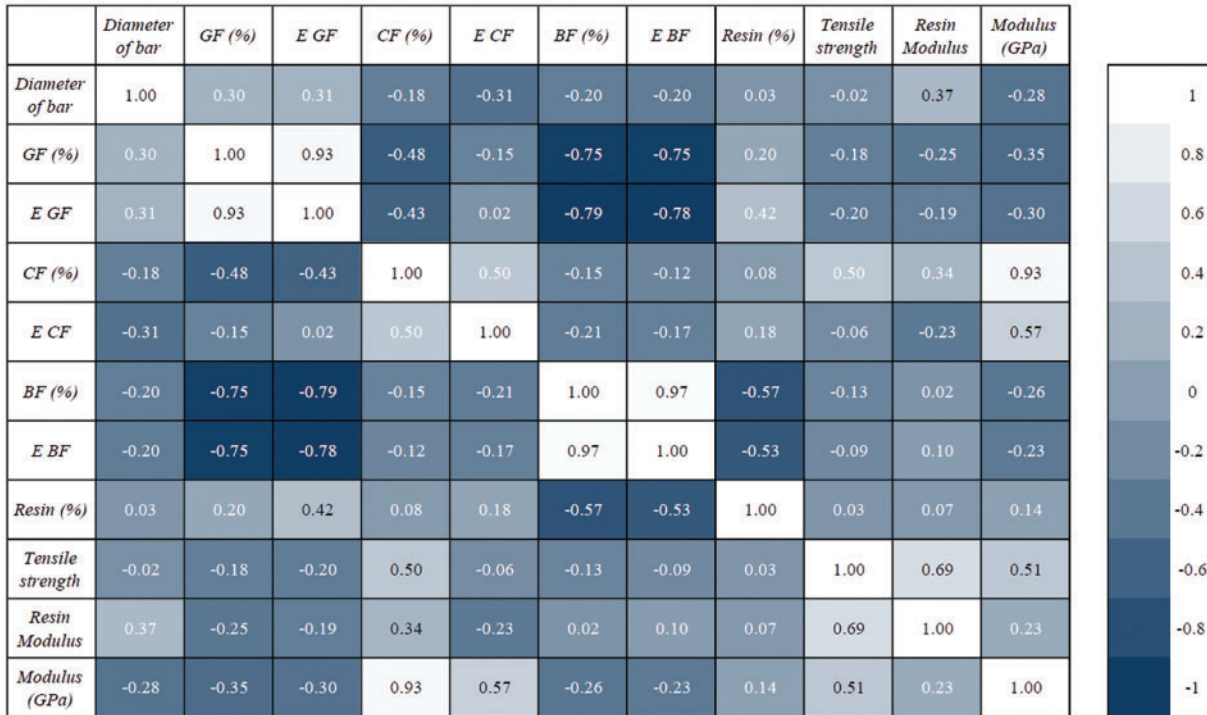


Figure 6: Pearson correlation matrix of the dataset

5.2 Model Development

GeneXproTool 5.0, a flexible GEP data modeling software, was used to predict the HFRP modulus of elasticity. This tool allows for the adjustment of various parameters, facilitating the creation of diverse GEP models with different characteristics. Table 4 presents a comprehensive GEP prediction model for HFRP elastic modulus, each configuration corresponds to a unique GEP setup identified by a code. For instance, “C25-G1-Addition” shows 25 chromosomes, 1 gene per chromosome, and addition as the linking function. The chromosome count remains consistent at 25, 50, 75, and 100 in each configuration. Additionally, all configurations have 8 genes per chromosome, influencing the overall model behavior. The linking function determines gene combinations within chromosomes, denoted by symbols such as “+”, “-”, “*”, “/”, or “Average,” representing addition, subtraction, multiplication, division, or averaging of input variables.

Table 4: GEP model development details

GEP model	Model details			
	Chromosomes	Head size	Genes	Linking function
C25-G1-Addition	25	8	1	+
C25-G1-Average	25	8	1	Average

(Continued)

Table 4 (continued)

GEP model	Chromosomes	Model details		
		Head size	Genes	Linking function
C25-G1-Division	25	8	1	/
C25-G1-Multiplication	25	8	1	*
C25-G1-Subtraction	25	8	1	-
C50-G1-Addition	50	8	1	+
C50-G1-Average	50	8	1	Average
C50-G1-Division	50	8	1	/
C50-G1-Multiplication	50	8	1	*
C50-G1-Subtraction	50	8	1	-
C75-G1-Addition	75	8	1	+
C75-G1-Average	75	8	1	Average
C75-G1-Division	75	8	1	/
C75-G1-Multiplication	75	8	1	*
C75-G1-Subtraction	75	8	1	-
C100-G1-Addition	100	8	1	+
C100-G1-Average	100	8	1	Average
C100-G1-Division	100	8	1	/
C100-G1-Multiplication	100	8	1	*
C100-G1-Subtraction	100	8	1	-

6 Model Evaluation Criteria

6.1 Statistical Metrics

The statistical performance of the proposed GEP models to predict MOE was measured using four analytical standard measures including the coefficient of determination (R^2), root relative squared error ($RRSE$), Root mean squared error ($RMSE$) and mean absolute error (MAE) [96–98]. The equation of each fitness measure is shown in Table 5. The best-fitted predictive model is usually based on the parameters. R^2 represents the proportion of the variance in the dependent variable (predicted from the independent variables). Therefore, the fitness of a regression model measures how well the model fits the observed data points [99,100]. $RRSE$ measures the standard deviation of the errors in a prediction model, relative to the range of the target variable. Therefore, the average difference between the predicted and actual values is normalized by the range of the target variable [96]. $RMSE$ measures the average magnitude of the errors in a prediction model. It represents the squared differences between the predicted and actual values [101–103]. MAE measures the average magnitude of the errors in a prediction model. It represents the absolute differences between the predicted and actual values [104].

Table 5: Models evaluation

Equation	Preferred fitness	Range
$RRSE = \sqrt{\frac{\sum_{i=1}^m (P_i - T_i)^2}{\sum_{i=1}^m (P_i - \bar{T})^2}}$	A lower value indicates better accuracy	0–∞

(Continued)

Table 5 (continued)

Equation	Preferred fitness	Range
$RMSE = \sqrt{\frac{\sum_{i=1}^m (P_i - T_i)^2}{m}}$	A lower value indicates better accuracy	0–∞
$MAE = \frac{1}{m} \sum_{i=1}^m P_i - T_i $	A lower value indicates better accuracy	0–∞
$R^2 = 1 - \frac{\sum_{i=1}^n (P_i - T_i)^2}{\sum_{i=1}^n (P_i - T_i)}$	A higher value indicates a better fit	0–1

Note: P_i is the predictive value and T_i is the targeting value.

6.2 K-Fold Cross-Validation

To assess the machine learning model’s flexibility and performance, the Cross-Validation (CV) technique is used. Various CV techniques, such as the Monte Carlo test, Jack Knife test, bootstrapping, three-way split cross-validation, and disjoint sets test, are utilized [105]. However, among these techniques, K-fold cross-validation (CV) is the most unbiased approach to address sampling and overfitting concerns.

The dataset is divided into “K” equal subsets to assess the model’s accuracy. The K-fold CV methodology creates K-1 subsets for training and one subset for testing to validate the training dataset [106]. This process is repeated K times with different data samples for training and testing. The best model is chosen based on approximation statistics for other errors from all the datasets. K-fold CV ensures complete dataset validation to obtain the most optimal model. The following steps are followed in K-fold validation: The dataset is divided into “K” equal subsets, where K-1 subsets are used for training, and one subset is reserved for testing and validation. The best model is developed from the K-1 subsets and validated on the remaining subset, considering all training subsets. The complete flow diagram of the K-fold CV algorithm is shown in Fig. 7.

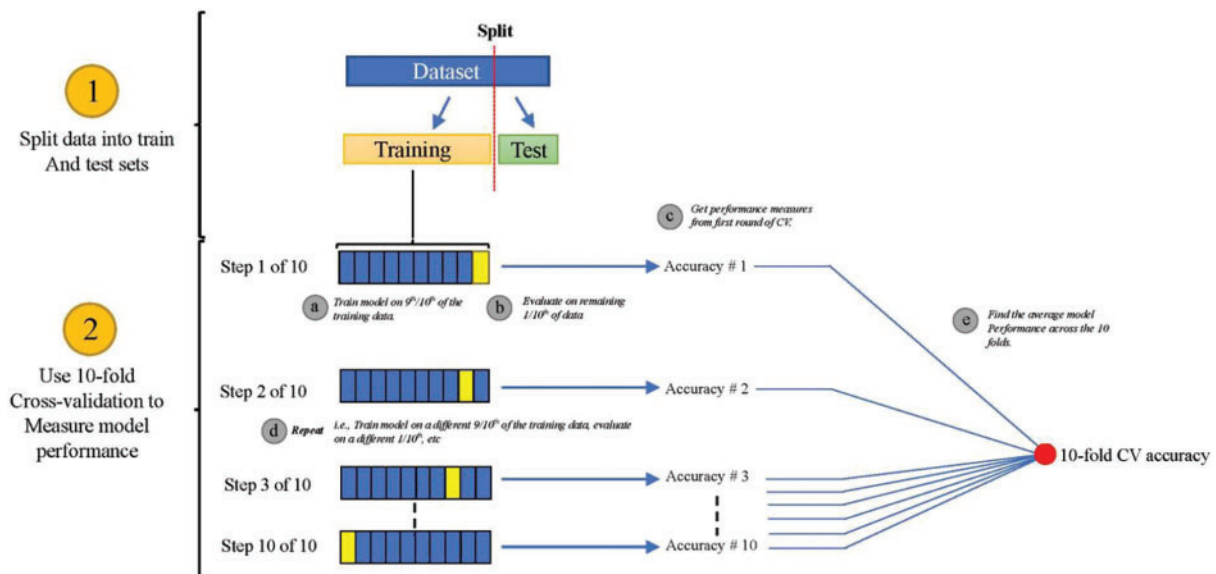


Figure 7: K-fold cross-validation flow diagram

7 Results and Discussion

Table 6 shows the different GEP models using various evaluation metrics for training and testing. The R^2 , RMSE, MAE, and RRSE values for each model are used for accuracy. The “C100-G1-Addition” model demonstrates better performance than models with an R^2 value of 0.96 in training and 0.96 in testing. Therefore a strong correlation exists between predicted and actual values. The model shows the lowest RMSE of 5.59, indicating accurate predictions with minimal error. The MAE value of 3.87 also supports the models accuracy (average magnitude of errors). Finally, the RRSE value of 0.19 shows that the models performance is better than others, reflecting the normalized error relative to the target variables.

Table 6: GEP model results

GEP Model	Training				Testing			
	R^2	RMSE	MAE	RRSE	R^2	RMSE	MAE	RRSE
C25-G1-Addition	0.8978	8.872	6.304	0.3197	0.9604	5.684	4.142	0.2013
C25-G1-Average	0.8778	9.796	6.581	0.3529	0.9332	7.455	4.898	0.264
C25-G1-Division	0.8837	9.466	6.647	0.3411	0.9445	6.731	4.791	0.2384
C25-G1-Multiplication	0.8999	8.783	6.256	0.3164	0.9548	6.039	4.403	0.2138
C25-G1-Subtraction	0.8921	9.117	6.826	0.3285	0.9404	7.101	5.267	0.2514
C50-G1-Addition	0.8977	8.877	6.346	0.3198	0.9665	5.315	3.988	0.1882
C50-G1-Average	0.9003	8.764	6.309	0.3158	0.9585	5.846	4.373	0.2071
C50-G1-Division	0.8782	9.801	6.478	0.3531	0.937	7.273	4.731	0.2575
C50-G1-Multiplication	0.8884	9.272	6.982	0.3341	0.9456	6.655	5.423	0.2356
C50-G1-Subtraction	0.8899	9.211	6.443	0.3319	0.9527	6.193	4.336	0.2193
C75-G1-Addition	0.9053	8.539	6.016	0.3077	0.9605	5.722	4.206	0.2026
C75-G1-Average	0.8922	9.113	6.487	0.3283	0.9683	5.176	3.989	0.1833
C75-G1-Division	0.8954	8.977	6.403	0.3234	0.9511	6.282	4.866	0.2225
C75-G1-Multiplication	0.8803	9.601	6.899	0.3459	0.9371	7.217	5.618	0.2556
C75-G1-Subtraction	0.8977	8.879	6.299	0.3199	0.9443	6.725	4.451	0.2405
C100-G1-Addition	0.9627	5.625	3.874	0.1934	0.9683	5.126	4.017	0.1961
C100-G1-Average	0.8726	9.906	6.786	0.3569	0.9428	6.868	4.801	0.2432
C100-G1-Division	0.8849	9.454	6.247	0.3405	0.9339	7.414	4.853	0.2625
C100-G1-Multiplication	0.8934	9.062	6.221	0.3265	0.9627	5.537	3.855	0.1815
C100-G1-Subtraction	0.8864	9.362	6.636	0.3373	0.9371	7.284	4.837	0.2579

7.1 Proposed GEP Model

Numerous models were generated by adjusting various parameters in GeneXprotool such as the number of chromosomes, genes, and functions. Statistical parameters such as R^2 , MAE, RMSE, and RRSE were employed to evaluate the performance of the developed GEP models. The optimal fitness model, “C100-G1-Addition” shows better performance with R^2 values of 0.96 during training and 0.96 during testing. Additionally, the GEP regression plot and error distribution diagram are illustrated in Figs. 8 and 9, respectively. The solid lines represent the predicted value, while the markers (e.g., circles and squares) indicate the observed data points. The different colors distinguish between training and testing datasets. In Fig. 9a, the comparison of experimental and predicted values of the modulus of elasticity is illustrated. The blue markers represent the experimental data, while the orange markers

denote the predicted values from the GEP model. Each data point corresponds to a specific dataset, and the lines connecting the markers help visualize the trend and correlation between the experimental and predicted values. Fig. 9b represents the error value (difference between experimental and predicted values) for each dataset.

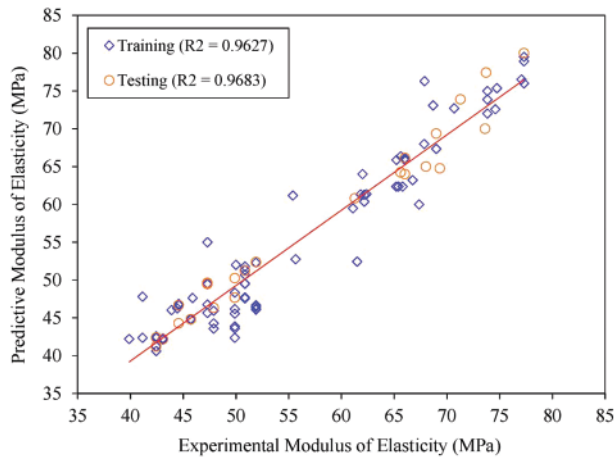


Figure 8: Regression plot

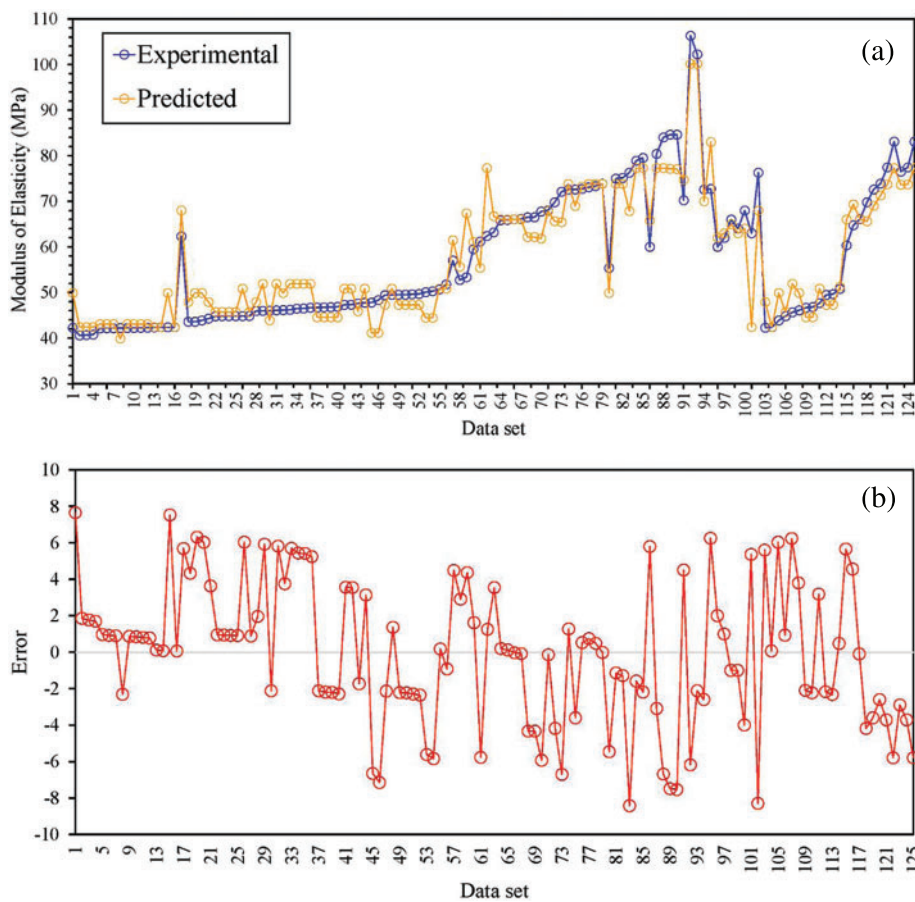


Figure 9: (a) Experimental vs. Predicted values (b) Error

The expression tree generated by GEP is from the best model “C100-G1-Addition” utilized to formulate the mathematical equation for the predictive model as shown in Fig. 10 and Eq. (2). This equation is for the utilization of a model generated by machine-learning techniques in the real world. By decoding the expression tree, a concise mathematical relationship between various input variables and mathematical operations (e.g., addition, subtraction, multiplication, division) is established. This simplified equation enables the calculation of the modulus of elasticity for HFRP bars.

$$E_{HFRP} = \frac{3BF_{\%}BF_E + GF_{\%}GF_E}{(10.6 - d - BF_{\%}BF_E)(CF_{\%}CF_E + GF_{\%}GF_E - 34.77)} + 0.68CF_{\%}CF_E - d + \frac{0.5}{M_{\%}M_tM_E} + 57.81 \tag{2}$$

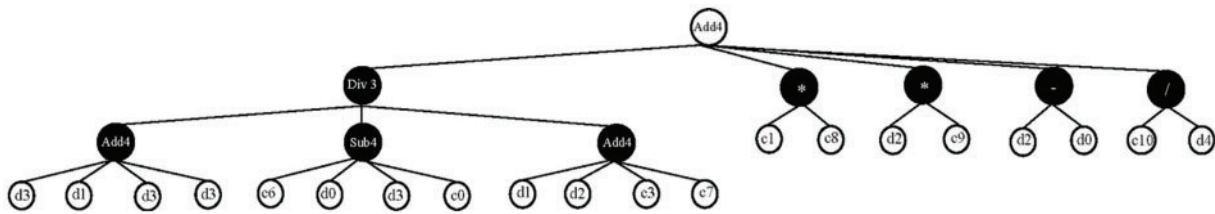


Figure 10: Expression tree of model “C100-G1-Addition”

7.2 K-Fold Cross-Validation

In this study, a 10-fold cross-validation technique was utilized to assess the performance of a predictive model. Cross-validation is a widely employed method in machine learning and statistical analysis to evaluate a model’s generalization capability. Fig. 11 illustrates the performance of the predictive model across the 10-fold cross-validation iterations.

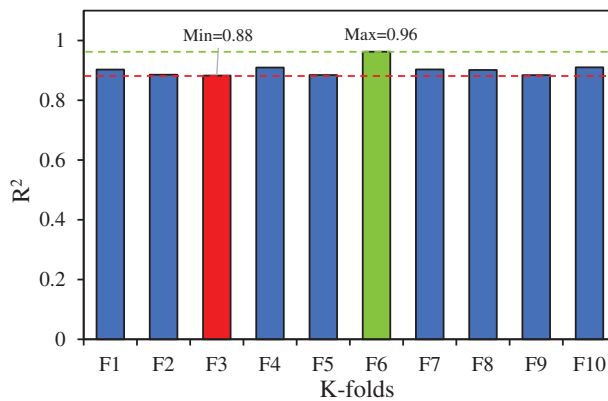


Figure 11: GEP model K-fold cross-validation results, R²

8 Parametric Analysis

Fig. 12 illustrates the correlations between the elastic modulus of hybrid fiber-reinforced polymer (HFRP) bars and each variable such as bar diameter, carbon fiber percentages, the elastic modulus of carbon fibers, the elastic modulus of basalt fibers, basalt fibers percentages, the elastic modulus of glass fibers, glass fibers percentages, resin matrix percentages, resin modulus, and tensile strength. It can be observed that all the variables positively influence the elastic modulus of HFRP bars. The discovered beneficial impacts of each variable on the elastic modulus of HFRP bars indicate that

changes in each parameter lead to an increase in the elastic modulus of the HFRP bars. Furthermore, the tensile strength more effectively increased the elastic modulus of HFRP bars than the other variables. These findings indicate that increasing the tensile capacity of concrete is a very effective approach to increasing its elastic modulus. Therefore, the study recommends that special attention should be given to the tensile strength to ensure better elastic modulus of HFRP bars. Also, it can be observed that each variable (other than tensile strength) has a significant role in increasing the elastic modulus of HFRP bars. Therefore, optimizing all the considered variables leads to an increase in the elastic modulus of the HFRP bars. These results have implications for carrying out efficient parametric studies and improving the design and manufacturing processes of HFRP bars to fulfill precise structural criteria.

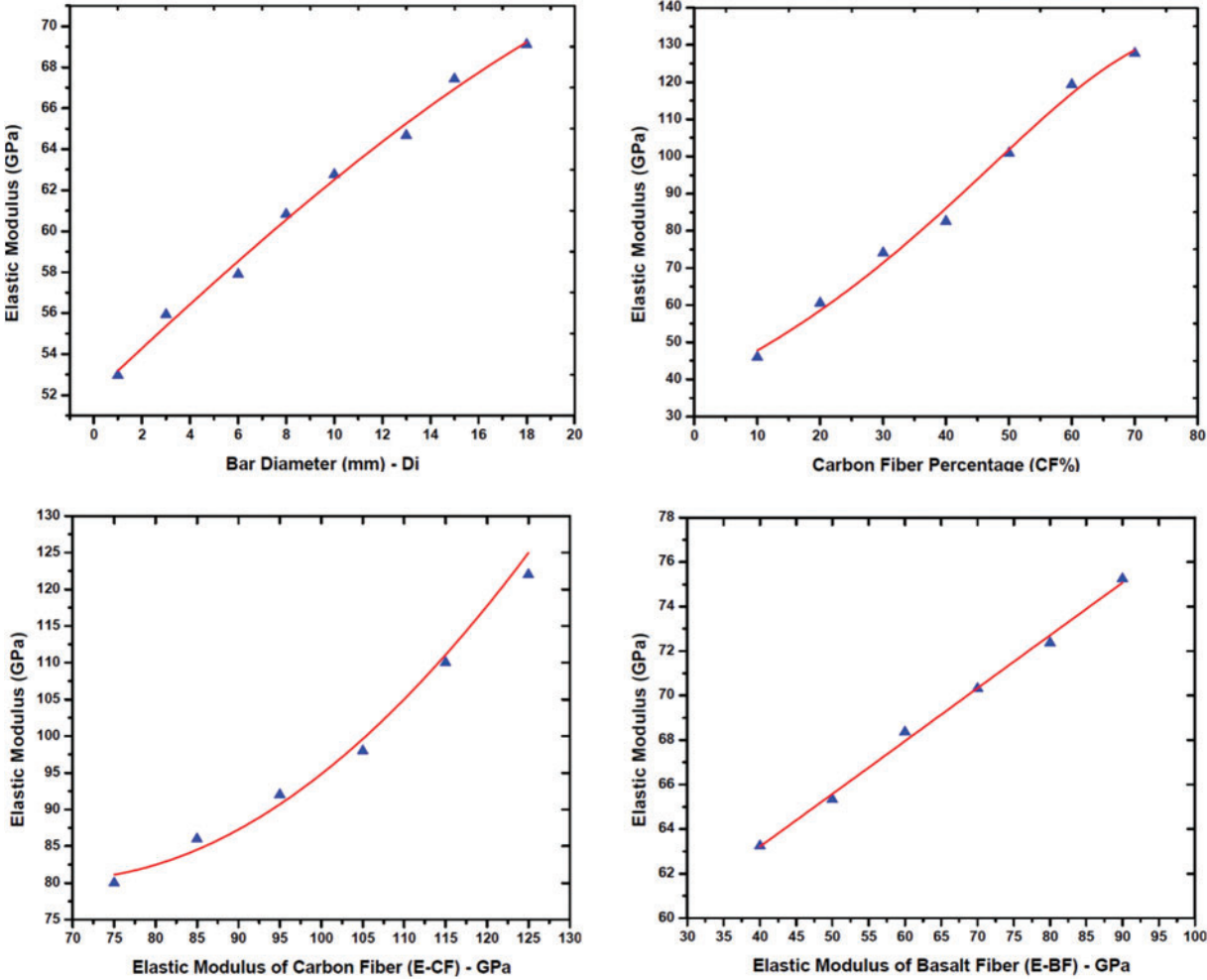


Figure 12: (Continued)

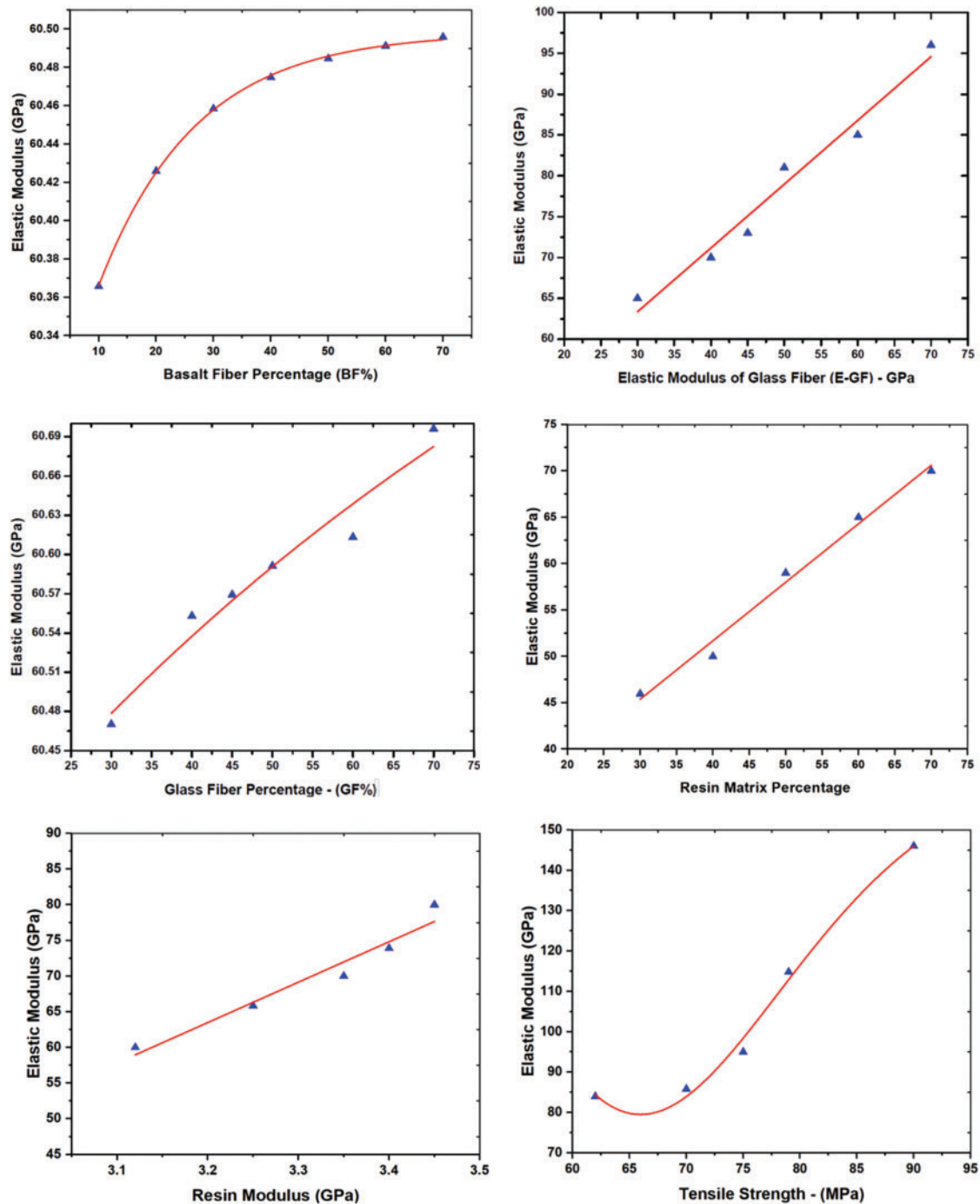


Figure 12: Parametric analysis

9 SHAP Analysis

The Shapley additive explanation (SHAP) framework provides internal and external explanations for investigating a critical variable. It is particularly suitable for collective machine learning techniques due to its robustness and ability to offer qualitative and quantitative insights, comparable to widely used feature significance metrics. In Fig. 13, prominent attributes significant contributions to the model's output, notably tensile strength, CF%, GF%, bar diameter, elastic modulus GF, resin%,

BF% and elastic modulus CF, resin modulus and elastic modulus BF influencing the prediction of elastic modulus. These influential parameters display distinct thresholds dictating their effects on the model's output. The intensity of each variable is judged through different colors. The red color indicates a highly sensitive variable that significantly impacts the elastic modulus. The SHAP analysis indicates that tensile strength is the most sensitive variable which significantly impacts the elastic modulus. Therefore, the study suggests that special attention should be given to the tensile strength while designing hybrid fiber-reinforced polymer (HFRP) bars.

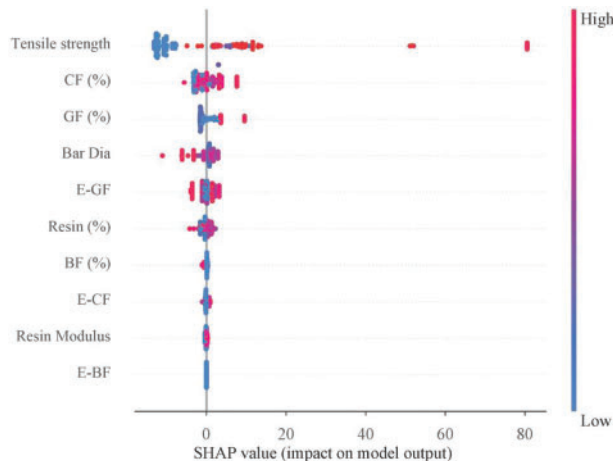


Figure 13: SHAP analysis

10 Comparative Analysis of GEP and Traditional Prediction Formula

Fig. 14 shows the comparison between the developed models of the GEP and the traditional prediction formula (ROM) available for elastic modulus. The alignment between the GEP model and experimental values is comparable. However considerable variation was noted between the experimental results and ROM value. Therefore, the findings indicate that the developed GEP model captures the patterns and relationships more accurately than the ROM model.

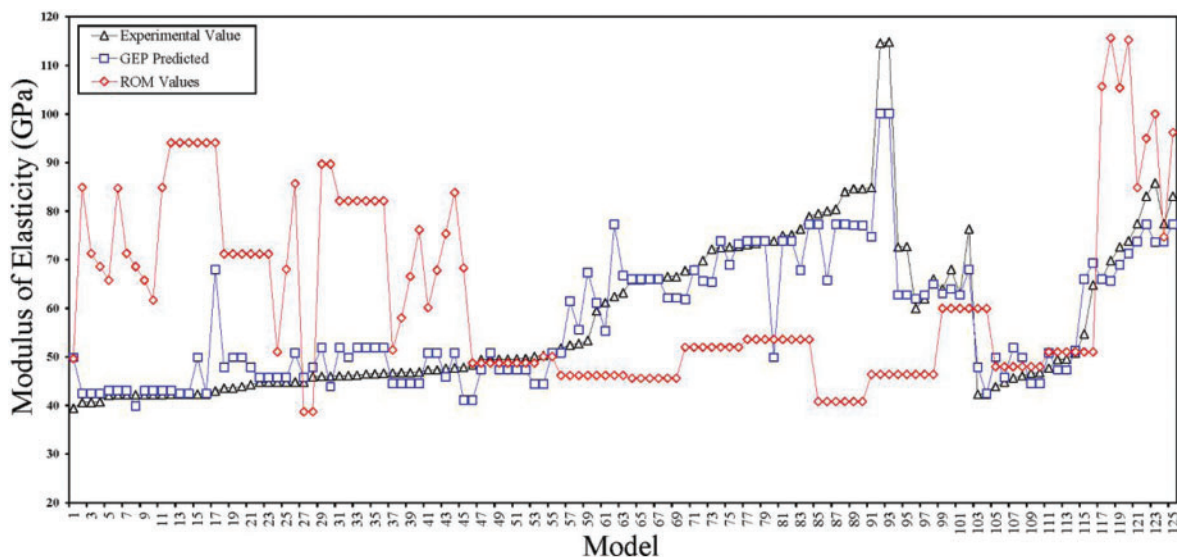


Figure 14: Comparison between results

11 Conclusion

The application of machine learning was applied to develop a predictive model for the elastic modulus of HFRP bars. A dataset containing 125 experimental results of HFRP bars was collected from the literature and used for model development and validation. The detailed conclusions are:

- The developed GEP model performance is better than the traditional available formula for predicting the elastic modulus of HFRP bars.
- A more accurate model (optimal predictive model) was identified with 100 chromosomes, 1 gene and an addition linking function.
- The statistical parameters such as R^2 , RMSE, MAE, and RRSE values are 0.96, 5.62, 3.87, and 0.1934, respectively, for training, and 0.96, 5.12, 4.01, and 0.196 for testing, respectively.
- A simplified mathematical equation for predicting the elastic modulus of HFRP bars is developed which offers a more straightforward approach for practical applications.
- Parametric and SHAP analyses identify tensile strength, carbon fiber, and glass fiber were the most significant contributing factors.
- Validation was performed through K-fold cross-validation (CV), demonstrating satisfactory performance across all models and further confirming the accuracy and reliability.

12 Limitations and Recommendations

Although the study provides promising results. However, the study has certain limitations and recommends future work to improve performance and accuracy.

- The study focused primarily on the prediction of the elastic modulus of HFRP bars. However, it might be possible that HFRP other properties like tensile strength and flexural behaviour influence overall performance. The study recommends future studies to explore different properties.
- Gene expression programming (GEP) was employed for predictive modelling and accuracy could be increased with the use of advanced algorithms. Therefore, the study recommends some advanced algorithms such as random forest or XGBoost to improve accuracy.
- Although the dataset used in this study is compressive, the variation in testing conditions, material properties, and fabrication methods may still have limitations. Therefore, the study recommends detailed controlled and standardized studies.

Acknowledgement: The authors gratefully acknowledge Zhengzhou University for providing the support and resources that enabled this research.

Funding Statement: The authors received no specific funding for this study.

Author Contributions: **Aneel Manan:** Software, Data curation, Visualization, Conceptualization, Methodology, Writing–original draft. **Pu Zhang:** Supervision, Methodology, Writing–review and editing. **Shoab Ahmad:** Investigation, Conceptualization, Formal analysis, Writing–review and editing. **Jawad Ahmad:** Conceptualization, Methodology, Data curation, Visualization, Writing–review and editing. All authors reviewed the results and approved the final version of the manuscript.

Availability of Data and Materials: Data will be made available upon request.

Ethics Approval: Not applicable.

Conflicts of Interest: The authors declare that they have no known competing financial interests or personal relationships that could have appeared to influence the work reported in this paper.

References

1. Pang B, Jin Z, Zhang Y, Xu L, Li M, Wang C, et al. Ultraductile waterborne epoxy-concrete composite repair material: epoxy-fiber synergistic effect on flexural and tensile performance. *Cem Concr Compos.* 2022;129:104463.
2. Li Z, Gao M, Lei Z, Tong L, Sun J, Wang Y, et al. Ternary cementless composite based on red mud, ultra-fine fly ash, and GGBS: synergistic utilization and geopolymerization mechanism. *Case Stud Constr Mater.* 2023;19:e02410.
3. Adeola OO, Tauheed Alfa M. The role of advance composite material in contemporary buildings. *J Contemp Urban Aff.* 2018;2(3):95–101. doi:10.25034/ijcua.2018.4723.
4. Attiogbe EK. Compliance concept in protection of concrete from freezing-and-thawing damage. *ACI Mater J.* 2020;117(6):187–200. doi:10.14359/51726995.
5. Nedeljković M, Visser J, Šavija B, Valcke S, Schlangen E. Use of fine recycled concrete aggregates in concrete: a critical review. *J Build Eng.* 2021;38(1):102196. doi:10.1016/j.jobe.2021.102196.
6. Santa AC, Tamayo JA, Correa CD, Gómez MA, Castaño JG, Baena LM. Atmospheric corrosion maps as a tool for designing and maintaining building materials: a review. *Heliyon.* 2022;8(9):e10438. doi:10.1016/j.heliyon.2022.e10438.
7. Taffese WZ, Sistonen E. Machine learning for durability and service-life assessment of reinforced concrete structures: recent advances and future directions. *Autom Constr.* 2017;77:1–14. doi:10.1016/j.autcon.2017.01.016.
8. Bhagwat Y, Nayak G, Lakshmi A, Pandit P. Corrosion of reinforcing bar in RCC structures—A review. *Lect Notes Civ Eng.* 2022;162(2):813–26. doi:10.1007/978-981-16-2826-9_51.
9. Li H, Yang Y, Wang X, Tang H. Effects of the position and chloride-induced corrosion of strand on bonding behavior between the steel strand and concrete. In: *Structures.* Amsterdam, Netherlands: Elsevier; 2023. vol. 58, p. 105500.
10. Li H, He G, Zhao Z, Liu Q, Wang J, Yin Y, et al. Abrasion performance and failure mechanism of fiber yarns based on molecular segmental differences. *J Eng Fiber Fabr.* 2024;19. doi:10.1177/15589250241228263.
11. Naser MZ, Hawileh RA, Abdalla JA. Fiber-reinforced polymer composites in strengthening reinforced concrete structures: a critical review. *Eng Struct.* 2019;198(12):109542. doi:10.1016/j.engstruct.2019.109542.
12. Sun L, Wang C, Zhang C, Yang Z, Li C, Qiao P. Experimental investigation on the bond performance of sea sand coral concrete with FRP bar reinforcement for marine environments. *Adv Struct Eng.* 2023;26(3):533–46. doi:10.1177/13694332221131153.
13. Cao J, Du J, Fan Q, Yang J, Bao C, Liu Y. Reinforcement for earthquake-damaged glued-laminated timber knee-braced frames with self-tapping screws and CFRP fabric. *Eng Struct.* 2024;306(6):117787. doi:10.1016/j.engstruct.2024.117787.
14. Guo F, Al-Saadi S, Singh Raman RK, Zhao XL. Durability of fiber reinforced polymer (FRP) in simulated seawater sea sand concrete (SWSSC) environment. *Corros Sci.* 2018;141:1–13. doi:10.1016/j.corsci.2018.06.022.
15. Li J. Application of corrosion resistance of FRP composites rebar in sea water sea sand concrete. *Appl Comput Eng.* 2023;7(1):131–5. doi:10.54254/2755-2721/7/20230401.
16. Khalifa A, Nanni A. Rehabilitation of rectangular simply supported RC beams with shear deficiencies using CFRP composites. *Constr Build Mater.* 2002;16(3):135–46. doi:10.1016/S0950-0618(02)00002-8.
17. Abdalla HA. Evaluation of deflection in concrete members reinforced with fibre reinforced polymer (FRP) bars. *Compos Struct.* 2002;56(1):63–71. doi:10.1016/S0263-8223(01)00188-X.
18. Ferreira AJM, Camanho PP, Marques AT, Fernandes AA. Modelling of concrete beams reinforced with FRP re-bars. *Compos Struct.* 2001;53(1):107–16. doi:10.1016/S0263-8223(00)00182-3.
19. Huang H, Yuan Y, Zhang W, Zhu L. Property assessment of high-performance concrete containing three types of fibers. *Int J Concr Struct Mater.* 2021;15(1):1–17. doi:10.1186/s40069-021-00476-7.
20. Chaallal O, Benmokrane B. Fiber-reinforced plastic rebars for concrete applications. *Compos Part B Eng.* 1996;27(3–4):245–52. doi:10.1016/1359-8368(95)00023-2.

21. Zhu H, Li C, Cheng S, Yuan J. Flexural performance of concrete beams reinforced with continuous FRP bars and discrete steel fibers under cyclic loads. *Polymers*. 2022;14(7):1399. doi:10.3390/polym14071399.
22. Benmokrane B, Chaallal O, Masmoudi R. Flexural response of concrete beams reinforced with FRP reinforcing bars. *ACI Struct J*. 1996;93(1):46–55. doi:10.14359/9839.
23. Sirimontree S, Keawsawasvong S, Thongchom C. Flexural behavior of concrete beam reinforced with GFRP bars compared to concrete beam reinforced with conventional steel reinforcements. *J Appl Sci Eng*. 2021;24(6). doi:10.6180/jase.202112_24(6).0009.
24. Xiao SH, Lin JX, Li LJ, Guo YC, Zeng JJ, Xie ZH, et al. Experimental study on flexural behavior of concrete beam reinforced with GFRP and steel-fiber composite bars. *J Build Eng*. 2021;43(13):103087. doi:10.1016/j.job.2021.103087.
25. Nanni A, de Luca A, Zadeh HJ. Reinforced concrete with FRP bars: mechanics and design. 2014. Available from: <https://www.afzir.com/knowledge/wp-content/uploads/2018/08/Nanni-A.-Reinforced-Concrete-with-FRP-Bars-Mechanics-and-Design-2014.pdf>. [Accessed 2024].
26. Schutte CL. Environmental durability of glass-fiber composites. *Mater Sci Eng R*. 1994;13(7):265–323. doi:10.1016/0927-796X(94)90002-7.
27. Wang H, Belarbi A. Ductility characteristics of fiber-reinforced-concrete beams reinforced with FRP rebars. *Constr Build Mater*. 2011;25(5):2391–401. doi:10.1016/j.conbuildmat.2010.11.040.
28. Matos B, Correia JR, Castro LMS, França P. Structural response of hyperstatic concrete beams reinforced with GFRP bars: effect of increasing concrete confinement. *Compos Struct*. 2012;94(3):1200–10. doi:10.1016/j.compstruct.2011.10.021.
29. Mousavi SR, Esfahani MR. Effective moment of inertia prediction of FRP-reinforced concrete beams based on experimental results. *J Compos Constr*. 2012;16(5):490–8. doi:10.1061/(asce)cc.1943-5614.0000284.
30. Feng G, Zhu D, Guo S, Rahman MZ, Jin Z, Shi C. A review on mechanical properties and deterioration mechanisms of FRP bars under severe environmental and loading conditions. *Cem Concr Compos*. 2022;134(24):104758. doi:10.1016/j.cemconcomp.2022.104758.
31. Hayashi T. On the improvement of mechanical properties of composites by hybrid composition. In: *Proceedings of 8th International Reinforced Plastics Conference*; 1972; London, England. p. 149–52.
32. Belarbi A, Chandrashekhara K, Watkins SE. Smart composite rebars with enhanced ductility. *Proc Eng Mech*. 1996;42(3):245–50.
33. Ali NM, Wang X, Wu Z. Integrated performance of FRP tendons with fiber hybridization. *J Compos Constr*. 2014;18(3):A4013007. doi:10.1061/(asce)cc.1943-5614.0000427.
34. Bakis CE, Nanni A, Terosky JA, Koehler SW. Self-monitoring, pseudo-ductile, hybrid FRP reinforcement rods for concrete applications. *Compos Sci Technol*. 2001;61(6):815–23. doi:10.1016/S0266-3538(00)00184-6.
35. Cui YH, Tao J. A new type of ductile composite reinforcing bar with high tensile elastic modulus for use in reinforced concrete structures. *Can J Civ Eng*. 2009;36(4):672–5. doi:10.1139/L09-012.
36. You YJ, Park YH, Kim HY, Park JS. Hybrid effect on tensile properties of FRP rods with various material compositions. *Compos Struct*. 2007;80(1):117–22. doi:10.1016/j.compstruct.2006.04.065.
37. Harris HG, Somboonsong W, Ko FK. New ductile hybrid FRP reinforcing bar for concrete structures. *J Compos Constr*. 1998;2(1):1–28. doi:10.1061/(ASCE)1090-0268(1998)2:1(28).
38. Wang S, Xia P, Chen K, Gong F, Wang H, Wang Q, et al. Prediction and optimization model of sustainable concrete properties using machine learning, deep learning and swarm intelligence: a review. *J Build Eng*. 2023;80:108065.
39. Lu B, Xia Y, Ren Y, Xie M, Zhou L, Vinai G, et al. When machine learning meets 2D materials: a review. *Adv Sci*. 2024;11(13):2305277.
40. Hu T, Zhang H, Cheng C, Li H, Zhou J. Explainable machine learning: compressive strength prediction of FRP-confined concrete column. *Mater Today Commun*. 2024;39(4):108883. doi:10.1016/j.mtcomm.2024.108883.
41. Cheng C, Taffese WZ, Hu T. Accurate prediction of punching shear strength of steel fiber-reinforced concrete slabs: a machine learning approach with data augmentation and explainability. *Buildings*. 2024;14(5):1223. doi:10.3390/buildings14051223.

42. Angelis D, Sofos F, Karakasidis TE. Artificial intelligence in physical sciences: symbolic regression trends and perspectives. *Arch Comput Methods Eng.* 2023;30(6):3845–65. doi:10.1007/s11831-023-09922-z.
43. Yao X, Lyu X, Sun J, Wang B, Wang Y, Yang M, et al. AI-based performance prediction for 3D-printed concrete considering anisotropy and steam curing condition. *Constr Build Mater.* 2023;375:130898.
44. Alyousef R, Rehman MF, Khan M, Fawad M, Khan AU, Hassan AM, et al. Machine learning-driven predictive models for compressive strength of steel fiber reinforced concrete subjected to high temperatures. *Case Stud Constr Mater.* 2023;19:e02418.
45. Alarfaj M, Qureshi HJ, Shahab MZ, Javed MF, Arifuzzaman M, Gamil Y. Machine learning based prediction models for spilt tensile strength of fiber reinforced recycled aggregate concrete. *Case Stud Constr Mater.* 2024;20:e02836.
46. Andersons J, Sparniņš E, Joffe R. Stiffness and strength of flax fiber/polymer matrix composites. *Polym Compos.* 2006;27(2):221–9. doi:10.1002/pc.20184.
47. Affdl JCH, Kardos JL. The Halpin-Tsai equations: a review. *Polym Eng Sci.* 1976;16(5):344–52. doi:10.1002/pen.760160512.
48. Sandier SI, Orbey H. 9 Mixing and combining rules. In: Sengers JV, Kayser RF, Peters CJ, White HJ, editors. *Equations state fluids fluid mix.* Amsterdam, Netherlands: Elsevier; 2000. vol. 5, p. 321–57. doi:10.1016/S1874-5644(00)80020-X.
49. Tham MW, Fazita MN, Abdul Khalil HPS, Mahmud Zuhudi NZ, Jaafar M, Rizal S, et al. Tensile properties prediction of natural fibre composites using rule of mixtures: a review. *J Reinf Plast Compos.* 2019;38(5):211–48. doi:10.1177/0731684418813650.
50. Arib RMN, Sapuan SM, Ahmad MMHM, Paridah MT, Khairul Zaman HMD. Mechanical properties of pineapple leaf fibre reinforced polypropylene composites. *Mater Des.* 2006;27(5):391–6. doi:10.1016/j.matdes.2004.11.009.
51. Luo S, Netravali AN. Interfacial and mechanical properties of environment-friendly ‘green’ composites made from pineapple fibers and poly(hydroxybutyrate-co-valerate) resin. *J Mater Sci.* 1999;34(22):5449–56. doi:10.1023/A:1004791807509.
52. Hashemi S. Effect of temperature on tensile properties of injection moulded short glass fibre and glass bead filled ABS hybrids. *Express Polym Lett.* 2008;2(7):474–84. doi:10.3144/expresspolymlett.2008.57.
53. Mansor MR, Sapuan SM, Zainudin ES, Nuraini AA, Hambali A. Stiffness prediction of hybrid kenaf/glass fiber reinforced polypropylene composites using rule of mixtures (ROM) and rule of hybrid mixtures (RoHM). *J Polym Mater.* 2013;30(3):321–34.
54. Venkateshwaran N, Elayaperumal A, Sathiya GK. Prediction of tensile properties of hybrid-natural fiber composites. *Compos Part B Eng.* 2012;43(2):793–6. doi:10.1016/j.compositesb.2011.08.023.
55. Miwa M, Horiba N. Effects of fibre length on tensile strength of carbon/glass fibre hybrid composites. *J Mater Sci.* 1994;29(4):973–7. doi:10.1007/BF00351419.
56. Biagiotti J, Fiori S, Torre L, López-Manchado MA, Kenny JM. Mechanical properties of polypropylene matrix composites reinforced with natural fibers: a statistical approach. *Polym Compos.* 2004;25(1):26–36. doi:10.1002/pc.20002.
57. Mirbagheri J, Tajvidi M, Hermanson JC, Ghasemi I. Tensile properties of wood flour/kenaf fiber polypropylene hybrid composites. *J Appl Polym Sci.* 2007; doi:10.1002/app.26363.
58. Fu SY, Xu G, Mai YW. On the elastic modulus of hybrid particle/short-fiber/polymer composites. *Compos Part B Eng.* 2002;33(4):291–9. doi:10.1016/S1359-8368(02)00013-6.
59. Facca AG, Kortschot MT, Yan N. Predicting the elastic modulus of natural fibre reinforced thermoplastics. *Compos Part A Appl Sci Manuf.* 2006;37(10):1660–71. doi:10.1016/j.compositesa.2005.10.006.
60. López JP, Mutjé P, Angels Pèlach M, El Mansouri NE, Boufi S, Vilaseca F. Analysis of the tensile modulus of polypropylene composites reinforced with stone groundwood fibers. *BioResources.* 2012;7(1):1310–23. doi:10.15376/biores.7.1.1310-1323.
61. Liang JZ. Predictions of Young’s modulus of short inorganic fiber reinforced polymer composites. *Compos Part B Eng.* 2012;43(4):1763–6. doi:10.1016/j.compositesb.2012.01.010.
62. Wang HL, Yin ZY. High performance prediction of soil compaction parameters using multi expression programming. *Eng Geol.* 2020;276(5):105758. doi:10.1016/j.enggeo.2020.105758.

63. Baykasoğlu A, Öztaş A, Özbay E. Prediction and multi-objective optimization of high-strength concrete parameters via soft computing approaches. *Expert Syst Appl.* 2009;36(3):6145–55. doi:10.1016/j.eswa.2008.07.017.
64. Nematzadeh M, Shahmansouri AA, Fakoor M. Post-fire compressive strength of recycled PET aggregate concrete reinforced with steel fibers: optimization and prediction via RSM and GEP. *Constr Build Mater.* 2020;252(6):119057. doi:10.1016/j.conbuildmat.2020.119057.
65. Ilyas I, Zafar A, Javed MF, Farooq F, Aslam F, Musarat MA, et al. Forecasting strength of cfrp confined concrete using multi expression programming. *Materials.* 2021;14(23):7134. doi:10.3390/ma14237134.
66. Bian F, Li TH, Cong PS. Genetic programming. *Fenxi Huaxue.* 1998;926–31 (In Chinese).
67. Cheng ZL, Zhou WH, Garg A. Genetic programming model for estimating soil suction in shallow soil layers in the vicinity of a tree. *Eng Geol.* 2020;268(1):105506. doi:10.1016/j.enggeo.2020.105506.
68. Gandomi AH, Babanajad SK, Alavi AH, Farnam Y. Novel approach to strength modeling of concrete under triaxial compression. *J Mater Civ Eng.* 2012;24(9):1132–43. doi:10.1061/(ASCE)MT.1943-5533.0000494.
69. Gandomi AH, Yun GJ, Alavi AH. An evolutionary approach for modeling of shear strength of RC deep beams. *Mater Struct Constr.* 2013;46(12):2109–19. doi:10.1617/s11527-013-0039-z.
70. Gao W. A comprehensive review on identification of the geomaterial constitutive model using the computational intelligence method. *Adv Eng Inform.* 2018;38(3):420–40. doi:10.1016/j.aei.2018.08.021.
71. Ferreira C. Gene expression programming: a new adaptive algorithm for solving problems *Cândida.* *Complex Syst.* 2011;13(2):87–129.
72. Iqbal M, Zhang D, Jalal FE, Faisal Javed M. Computational AI prediction models for residual tensile strength of GFRP bars aged in the alkaline concrete environment. *Ocean Eng.* 2021;232(5):109134. doi:10.1016/j.oceaneng.2021.109134.
73. Chu HH, Khan MA, Javed M, Zafar A, Ijaz Khan M, Alabduljabbar H, et al. Sustainable use of fly-ash: use of gene-expression programming (GEP) and multi-expression programming (MEP) for forecasting the compressive strength geopolymer concrete. *Ain Shams Eng J.* 2021;12(4):3603–17. doi:10.1016/j.asej.2021.03.018.
74. Awoyera PO, Kirgiz MS, Viloría A, Ovallos-Gazabon D. Estimating strength properties of geopolymer self-compacting concrete using machine learning techniques. *J Mater Res Technol.* 2020;9(4):9016–28. doi:10.1016/j.jmrt.2020.06.008.
75. Khan MA, Zafar A, Akbar A, Javed MF, Mosavi A. Application of gene expression programming (GEP) for the prediction of compressive strength of geopolymer concrete. *Materials.* 2021;14(5):1106. doi:10.3390/ma14051106.
76. Farooq F, Nasir Amin M, Khan K, Rehan Sadiq M, Javed MF, Aslam F, et al. A comparative study of random forest and genetic engineering programming for the prediction of compressive strength of high strength concrete (HSC). *Appl Sci.* 2020;10(20):7330. doi:10.3390/app10207330.
77. Akin OO, Ocholi A, Abejide OS, Obari JA. Prediction of the compressive strength of concrete admixed with metakaolin using gene expression programming. *Adv Civ Eng.* 2020;2020(2):1–7. doi:10.1155/2020/8883412.
78. Awoyera PO, Mansouri I, Abraham A, Viloría A. A new formulation for strength characteristics of steel slag aggregate concrete using an artificial intelligence-based approach. *Comput Concr.* 2021;27(4):333–41. doi:10.12989/cac.2021.27.4.333.
79. Khan MA, Zafar A, Farooq F, Javed MF, Alyousef R, Alabduljabbar H, et al. Geopolymer concrete compressive strength via artificial neural network, adaptive neuro fuzzy interface system, and gene expression programming with k-fold cross validation. *Front Mater.* 2021;8:621163. doi:10.3389/fmats.2021.621163.
80. Ahmadi M, Kheyroddin A, Dalvand A, Kioumars M. New empirical approach for determining nominal shear capacity of steel fiber reinforced concrete beams. *Constr Build Mater.* 2020;234:117293. doi:10.1016/j.conbuildmat.2019.117293.
81. Mousavi M, Azarbakht A, Rahpeyma S, Farhadi A. On the application of genetic programming for new generation of ground motion prediction equations. *Handb Genet Program Appl.* 2015;38(1):309–43. doi:10.1007/978-3-319-20883-1_12.

82. Wang M, Wan W. A new empirical formula for evaluating uniaxial compressive strength using the Schmidt hammer test. *Int J Rock Mech Min Sci.* 2019;123(1):104094. doi:10.1016/j.ijrmmms.2019.104094.
83. Soleimani S, Rajaei S, Jiao P, Sabz A, Soheilinia S. New prediction models for unconfined compressive strength of geopolymer stabilized soil using multi-gen genetic programming. *Meas J Int Meas Confed.* 2018;113(23):99–107. doi:10.1016/j.measurement.2017.08.043.
84. Ferreira C. Mutation, transposition, and recombination: an analysis of the evolutionary dynamics. In: *Proceedings of the 6th Joint Conference on Information Science*; New York, USA; 2002.
85. Gandomi AH, Roke DA. Assessment of artificial neural network and genetic programming as predictive tools. *Adv Eng Softw.* 2015;88(3):63–72. doi:10.1016/j.advengsoft.2015.05.007.
86. Protchenko K, Zayoud F, Urbański M, Szmigiera E. Tensile and shear testing of basalt fiber reinforced polymer (BFRP) and hybrid basalt/carbon fiber reinforced polymer (HFRP) bars. *Materials.* 2020;13(24):5839. doi:10.3390/ma13245839.
87. Szmigiera ED, Protchenko K, Urbański M, Garbacz A. Mechanical properties of hybrid FRP bars and nano-hybrid FRP bars. *Arch Civ Eng.* 2019;65(1):97–110. doi:10.2478/ace-2019-0007.
88. Won JP, Park CG, Jang CII. Tensile fracture and bond properties of ductile hybrid FRP reinforcing bars. *Polym Polym Compos.* 2007;15(1):9–16. doi:10.1177/096739110701500102.
89. Gao D, Zhang Y, Wen F, Fang D, Pang Y, Tang J, et al. Design method and experiment verification for hybrid fiber reinforced polymer bars with both tensile ductility and different strength grades. *J Build Eng.* 2022;46(6):103723. doi:10.1016/j.job.2021.103723.
90. Gao D, Zhang Y, Pang Y, Wen F, Fang D, Tang J. Five-stage tensile constitutive model of hybrid fiber reinforced polymer bar. *J Build Eng.* 2022;58(1):105006. doi:10.1016/j.job.2022.105006.
91. Hiesch D, Proske T, Graubner CA, Bujotzek L, El Ghadioui R. Theoretical and experimental investigation of the time-dependent relaxation rates of GFRP and BFRP reinforcement bars. *Struct Concr.* 2023;24(2):2800–16. doi:10.1002/suco.202200212.
92. Youssef T, Benmokrane B. Creep behavior and tensile properties of GFRP bars under sustained service loads. *Am Concr Institute, ACI Spec Publ.* 2011. doi:10.14359/51682449.
93. Hitesh Kumar M, Mohandoss P, Anjana L. Investigation on tensile and creep behaviour of glass fiber reinforced polymer (GFRP) bars: a review. *Mater Today Proc.* 2023;7(2):194. doi:10.1016/j.matpr.2023.04.656.
94. Shi J, Wang X, Huang H, Wu Z. Relaxation behavior of prestressing basalt fiber-reinforced polymer tendons considering anchorage slippage. *J Compos Mater.* 2017;51(9):1275–84. doi:10.1177/0021998316673893.
95. Yang D, Zhang J, Song S, Zhou F, Wang C. Experimental investigation on the creep property of carbon fiber reinforced polymer tendons under high stress levels. *Materials.* 2018;11(11):2273. doi:10.3390/ma11112273.
96. Botchkarev A. A new typology design of performance metrics to measure errors in machine learning regression algorithms. *Interdiscip J Inf, Knowl, Manag.* 2019;14:45–76. doi:10.28945/4184.
97. Çanakci H, Baykasoğlu A, Güllü H. Prediction of compressive and tensile strength of Gaziantep basalts via neural networks and gene expression programming. *Neural Comput Appl.* 2009;18(8):1031–41. doi:10.1007/s00521-008-0208-0.
98. Iqbal MF, Liu QF, Azim I, Zhu X, Yang J, Javed MF, et al. Prediction of mechanical properties of green concrete incorporating waste foundry sand based on gene expression programming. *J Hazard Mater.* 2020;384:121322. doi:10.1016/j.jhazmat.2019.121322.
99. Alavi AH, Gandomi AH, Nejad HC, Mollahasani A, Rashed A. Design equations for prediction of pressuremeter soil deformation moduli utilizing expression programming systems. *Neural Comput Appl.* 2013;23(6):1771–86. doi:10.1007/s00521-012-1144-6.
100. Zhang W, Zhang R, Wu C, Goh ATC, Lacasse S, Liu Z, et al. State-of-the-art review of soft computing applications in underground excavations. *Geosci Front.* 2020;11(4):1095–106. doi:10.1016/j.gsf.2019.12.003.
101. Alade IO, Abd Rahman MA, Saleh TA. Modeling and prediction of the specific heat capacity of Al₂O₃/water nanofluids using hybrid genetic algorithm/support vector regression model. *Nano-Structures and Nano-Objects.* 2019;17:103–11. doi:10.1016/j.nanoso.2018.12.001.
102. Kisi O, Shiri J, Tombul M. Modeling rainfall-runoff process using soft computing techniques. *Comput Geosci.* 2013;51(2):108–17. doi:10.1016/j.cageo.2012.07.001.

103. Majidifard H, Jahangiri B, Rath P, Urrea Contreras L, Buttlar WG, Alavi AH. Developing a prediction model for rutting depth of asphalt mixtures using gene expression programming. *Constr Build Mater.* 2021;267(3):120543. doi:10.1016/j.conbuildmat.2020.120543.
104. Gandomi AH, Alavi AH, Mousavi M, Tabatabaei SM. A hybrid computational approach to derive new ground-motion prediction equations. *Eng Appl Artif Intell.* 2011;24(4):717–32. doi:10.1016/j.engappai.2011.01.005.
105. Wong TT, Yeh PY. Reliable accuracy estimates from k-fold cross validation. *IEEE Trans Knowl Data Eng.* 2020;32(8):1586–94. doi:10.1109/TKDE.2019.2912815.
106. Bengio Y, Grandvalet Y. No unbiased estimator of the variance of k-fold cross-validation. *J Mach Learn Res.* 2004;5:1089–105.